UC Irvine

Title

Global-scale variations of the ratios of carbon to phosphorus in exported marine organic matter

Permalink

https://escholarship.org/uc/item/3gx415pv

Journal

Nature Geoscience, 7(12)

ISSN

1752-0894

Authors

Teng, Yi-Cheng
Primeau, François W
Moore, J Keith
et al.

Publication Date

2014-12-01

DOI

10.1038/ngeo2303

Peer reviewed

Global-scale variations of the ratios of carbon to phosphorus in exported marine organic matter

Yi-Cheng Teng[1], François W. Primeau[1]*, J. Keith Moore[1], Michael W. Lomas[2] and Adam C. Martiny[1,3]

The ratio of carbon (C) to phosphorus (P) in marine phytoplankton is thought to be constant throughout the worlds' oceans. Known as the Redfield ratio[1], this relationship describes the links between carbon and phosphorus cycling and marine ecosystems[2–4]. However, variations in the stoichiometry of phytoplankton have recently been identified, in particular strong latitudinal variability[5]. Here we assess the impact of this variability in the C:P ratio of biomass on the C:P ratio of organic matter that is exported to the deep ocean using a biogeochemical inverse-model based on a data-constrained ocean circulation model[6,7] and a global database[8,9] of dissolved inorganic carbon and phosphate measurements. We identify global patterns of variability in the C:P ratios of exported organic matter, with higher values in the nutrient-depleted subtropical gyres, where organic matter export is relatively low, and lower ratios in nutrient-rich upwelling zones and high-latitude regions, where organic matter export is high. This suggests that total carbon export is relatively constant throughout the oceans, in agreement with recent estimates of carbon fluxes[10]. We conclude that the latitudinal patterns of C:P in exported organic matter are consistent with the large-scale stoichiometric variations in phytoplankton C:P. We suggest that a future expansion of nutrient-depleted waters could result in a shift to more efficient C export that compensates for the expected decline in productivity.

The remineralization at depth of organic matter produced in the surface ocean helps maintain a vertical gradient in dissolved inorganic carbon and nutrients against the homogenizing action of the overturning circulation. The presence of this gradient has profound impacts on the fertility of the ocean and the partitioning of carbon dioxide between the atmosphere and ocean[11]. To infer the C:P ratio of exported organic matter ($(C:P)_{exp}$) from the imprint it leaves on gradients of phosphate (PO_4) and dissolved inorganic carbon (DIC) during remineralization, one must account for the extensive mixing of water masses with different initial concentrations. Previous studies have been unable to detect reliable patterns of C:P variability[12–14]—perhaps due to limitations of the simple endmember mixing models[15]. Indeed, recent research has shown that the transport of preformed PO_4 and DIC from the surface to the interior involves the mixing of a continuous distribution of initial concentrations, which can only be accurately represented using many discrete endmembers[16]. To overcome these limitations, we formulated a biogeochemical inverse-model based on a data-constrained three-dimensional ocean circulation model that accurately represents the mixing and transport of water masses[6,7]. We coupled the circulation model to a biogeochemical model in which the C:P ratio of exported organic matter is an explicit parameter that varies across 11 surface regions chosen to separate the nutrient-depleted subtropical gyres from the nutrient-rich upwelling and high-latitude regions (Fig. 1). The resulting model allows us to infer the C:P ratio of exported organic matter using a Bayesian inversion procedure combined with a numerical optimization technique that finds the most probable $(C:P)_{exp}$ parameters conditioned on the PO_4 and DIC tracer observations (Methods and Supplementary Methods).

The inferred globally integrated $(C:P)_{exp}$ is equal to 105:1, and thus in close agreement with the canonical Redfield value of 106:1. However, we also see regional variation, whereby $(C:P)_{exp}$ ranges from a minimum of 63:1 in the sub-polar North Atlantic to a maximum of 355:1 in the subtropical North Atlantic (Fig. 1). The model with variable $(C:P)_{exp}$ improves the agreement between the simulated and observed DIC concentrations compared to the model with constant $(C:P)_{exp}$ set to the mean value of 105:1 (Fig. 2). The layer-averaged root mean squared (r.m.s.) error in the model with variable $(C:P)_{exp}$ is decreased by as much as 75% at ∼3,800 m and by 40% on average. This decrease in r.m.s. error over the whole water column implies that $(C:P)_{exp}$ is best represented by values unique to each region.

Our inverse model reveals elevated $(C:P)_{exp}$ values in the subtropical gyres and lower $(C:P)_{exp}$ values in the equatorial and high-latitude regions. If we assume that the low C:N ratio observed in high-latitude suspended particles[17] is also present in exported organic matter, the low $(C:P)_{exp}$ in high-latitude regions is consistent with the high-latitude dominance of diatoms, which have been shown to contribute export with low N:P ratios[18]. We also find extensive regional variation in $(C:P)_{exp}$ between the subtropical gyres. For example, the North Atlantic $(C:P)_{exp}$ is approximately twice that of the North Pacific subtropical gyre. A large difference is also observed in the C:P ratio of sinking particulate matter measured using sediment traps at the Bermuda Atlantic Time-series Study (BATS) and the Hawaii Ocean Time-series (HOT; Supplementary Fig. 1). We suggest that this difference is driven by the more extreme phosphorus limitation of the North Atlantic[19,20]. We also see an elevated ratio in the subtropical gyres of the Northern Hemisphere versus the Southern Hemisphere. We speculate that differences in $(C:P)_{exp}$ among subtropical gyres are linked to the degree of P stress, which is influenced by multiple factors—including basin-scale inputs of N, P and Fe, and basin-scale rates of nitrogen fixation and denitrification[21–23]. The strongest evidence for P-limitation is in the North Atlantic subtropical gyre[19], where we find the largest $(C:P)_{exp}$ and a maximum C:P in the bulk surface POM (ref. 5).

We next compared our inferred $(C:P)_{exp}$ to the ratio measured in suspended particles, $(C:P)_{particles}$ (ref. 5) and find that they show a remarkable degree of consistency (Fig. 3). Although the particulate

[1]Department of Earth System Science, University of California, Irvine, California 92697, USA. [2]Bigelow Laboratory for Ocean Sciences, East Boothbay, Maine 04544, USA. [3]Department of Ecology and Evolutionary Biology, University of California, Irvine, California 92697, USA. *e-mail: fprimeau@uci.edu
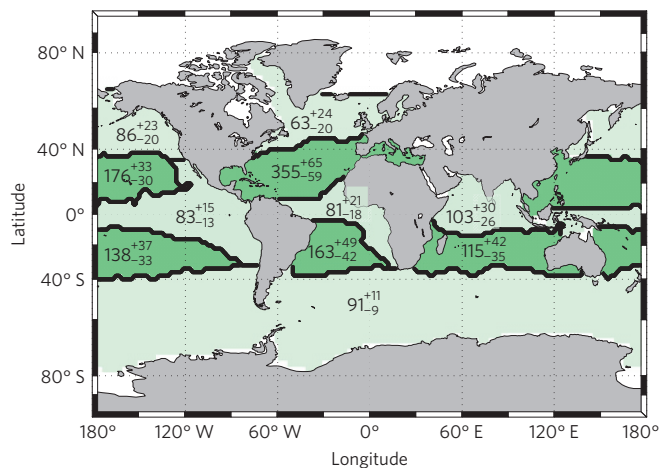
Figure 1 | Map of (C:P)$_{exp}$ values inferred from the inverse model.
The values correspond to the location of the maximum of the posterior
probability density function (pdf). The error bars correspond to ± 1
standard deviation of the posterior pdf. Nutrient-depleted subtropical
regions are indicated in dark green and nutrient-rich regions are indicated in
light green. The boundary separating the regions is based on the
$(0.3\ \text{mmol/m}^{-3})$-contour of the annually averaged PO_4 concentration. The
sensitivity of the inversion results to the choice of boundary threshold is
explored in Supplementary Methods and Supplementary Table 3.

**Figure 2 | Layer-averaged root mean squared (r.m.s.) DIC misfit
(μmol C kg^{-1}).** The red circles correspond to the spatially varying (C:P)$_{exp}$
model and the blue squares correspond to the constant (C:P)$_{exp}$ model.
Data for only the upper 2,000 m (shaded region) were used to optimize the
(C:P)$_{exp}$ parameters, but the improvement in the fit extends to the bottom
of the ocean. Further figures showing the model-data misfits are available in
Supplementary Figs 2 and 3.

measurements show considerable scatter, the available data suggest
that (C:P)$_{particles}$ is elevated in the subtropical gyres compared to
the tropical upwelling and sub-polar regions, in agreement with
our inverse-model estimates. It has been hypothesized that the
variability observed in plankton elemental ratios might be averaged
out by the seasonal succession of phytoplankton, or possibly by
trophic interactions[18]. The general agreement between the large-
scale variability in (C:P)$_{exp}$ and (C:P)$_{particles}$ is inconsistent with
the ecosystem-averaging hypothesis and suggests that the spatial
variations in the C:P ratio of exported organic material reflect the
C:P variability of phytoplankton. Furthermore, the high (C:P)$_{exp}$
values in the gyres indicate that oligotrophic ecosystems can make
an appreciable contribution to carbon export fluxes by more
efficiently using the limited P resource[24].

The spatial variability of (C:P)$_{exp}$ has important implications for
the spatial pattern of annual net community production (ANCP).
At present, satellite-derived estimates of ANCP are fairly uncertain,
but tend to show values that are at least a factor of two lower in the
subtropics compared to high latitudes[25,26]. In contrast to the satellite-
based estimates and those of most global ocean biogeochemical
models, the limited number of sites with experimental determina-
tions of ANCP indicate less variation[10]. We compare these experi-
mentally determined ANCP values against the export production
computed with either a constant (C:P)$_{exp}$ or the optimal spatially
varying (C:P)$_{exp}$ (Fig. 4). Both models have the same globally inte-
grated export production, but the model with a constant (C:P)$_{exp}$
underestimates carbon fluxes in the subtropical gyre sites (BATS
and HOT) by ~60% and overestimates carbon fluxes in the high-
latitude North Pacific site (OSP) by more than 40%. In contrast, the
carbon export fluxes estimated from the model with the variable
(C:P)$_{exp}$ are in agreement with the experimentally determined fluxes
at all locations. Particularly notable is the increase in the fraction
of the globally integrated carbon export for the subtropical North
Atlantic Ocean from ~3% for the fixed C:P = 105:1 model to 9%
for the variable stoichiometry model (Supplementary Fig. 4e,f). The
agreement of our estimates with the experimental determinations
points towards the need for continued evaluation of the satellite-
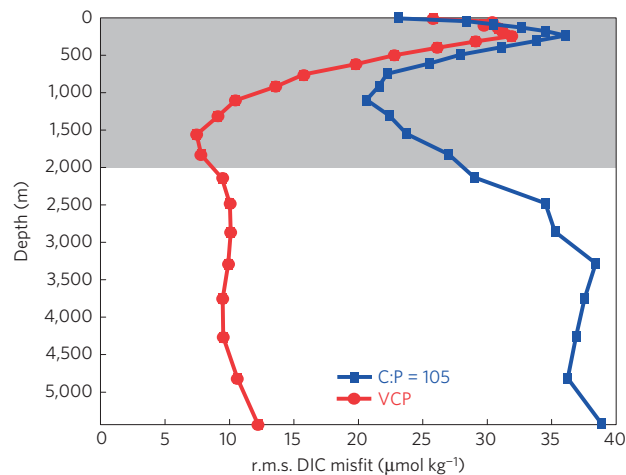based NCP estimation algorithms and for the need to implement

variable stoichiometry in marine biogeochemical models. If we use
our model to extrapolate the limited number of experimentally
determined ANCP values to the global ocean, the resulting spatial
pattern of export flux implies a more efficient biological carbon
pump in the subtropical gyres because the residence time of carbon
exported from subtropical gyres tends to be longer than that of
carbon exported from upwelling regions[27].

In this study we developed a new method for inferring (C:P)$_{exp}$
from PO_4 and DIC tracer data that uses a Bayesian inverse
method with a numerical optimization technique applied to a
global biogeochemical model coupled to a data-assimilated ocean
circulation model. The use of a three-dimensional model to
explicitly account for the dominant physical and biogeochemical
processes that maintain the climatological PO_4 and DIC gradients
greatly reduces the unexplained fraction of data variance. In
comparison to simple endmember mixing models, this new method
provides a more powerful technique for detecting the regional
(C:P)$_{exp}$ signal in the tracer data. However, it is important to consider
possible limitations of the model. In particular, the analysis assumes
that organic carbon and phosphorus remineralize at the same rate.
In support of this simplifying assumption, we find that the results
from this simpler model are qualitatively robust, when compared
to a model with element- and region-specific rates (Supplementary
Methods and Supplementary Figs 5–7). The inferred (C:P)$_{exp}$ from
both the complex and simpler models agree within two standard
deviations in all regions and within one standard deviation in
8 of the 11 regions. For the model with element- and region-
specific rates the remineralization C:P ratio tends to increase with
depth in most regions, but the general pattern of a higher C:P
ratio for material exported from nutrient-poor surface regions
persists with depth (Supplementary Fig. 6). Our model also assumes
that, apart from the invasion of anthropogenic carbon into the
ocean, the marine carbon and phosphorus cycles are in steady
state. This assumption is made because of the lack of data to the
contrary, but the possibility that global marine biogeochemical
cycles may not be stationary is something that needs to be explored
with prognostic biogeochemical models that allow for variable
elemental stoichiometry.

The general correspondence between patterns of C:P variability
in phytoplankton and in C:P variability of remineralization fluxes
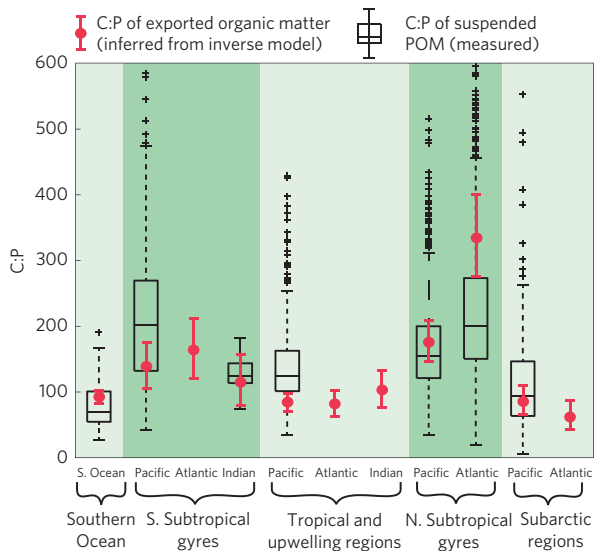
Figure 3 | Comparison of the C:P ratio of suspended particulate organic matter (POM) to that of exported organic matter. The C:P ratio of suspended POM data is from ref. 4 and comprises data for the upper 300 m of the water column binned into our 11 regions. The box plots show the 25, 50 and 75 percentiles, while the whiskers cover 99.3% of the data, with the remaining data points shown with '+' symbols. Values of $(C:P)_{exp}$ inferred from our geochemical inverse model are shown with error bars corresponding to the errors shown in Fig. 1.
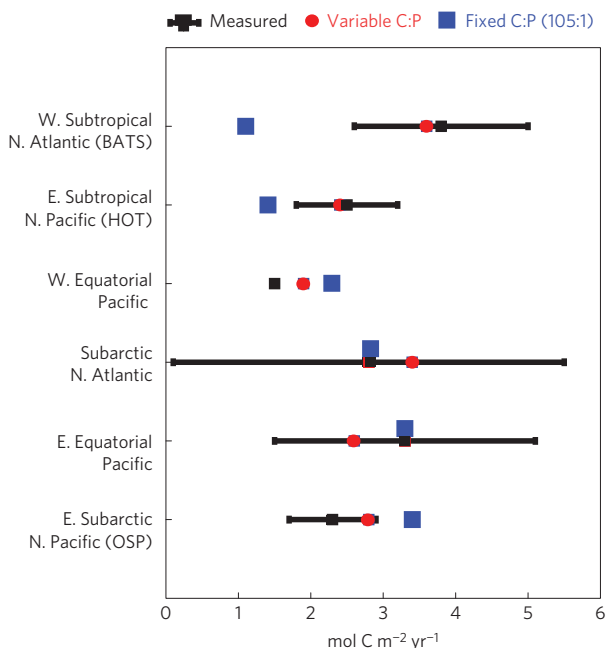

Figure 4 | Experimentally determined export production at six sites from Table 2 of ref. 9. Estimated carbon export calculated from our model using the distinct $(C:P)_{exp}$ values is shown as red circles and using a fixed $(C:P)_{exp} = 105:1$ is shown as blue squares. The model-derived export productions include export of POC and DOC with the DOC export referenced to the location where the biological production occurred, as opposed to where the DOC is subducted and mixed into the thermocline.

implies that shifts in plankton community or in resource allocation within species driven by climate change might result in changes in $(C:P)_{exp}$ that would produce potentially important feedbacks on

the Earth's carbon cycle and climate. Present Earth System Models (which assume fixed Redfield stoichiometry) suggest declines in carbon productivity and export over the twenty-first century, due in part to expanding oligotrophic regions[3,4,28]. Our results suggest that the more efficient carbon export in these regions would partially offset these expected declines in production and export.

Methods

Ocean circulation model. The circulation is based on the model of refs 6,7, which assimilates climatological observations of temperature, salinity, phosphate, natural radiocarbon, mean sea surface height, and air–sea heat and freshwater fluxes, as well as transient CFC-11 observations.

Biogeochemistry model. The biological uptake of phosphorus is modelled using

$$J_P = \gamma \cdot [PO_4]$$

where $[PO_4]$ is the model phosphate concentration and γ is a rate coefficient estimated empirically from satellite-derived net primary production (NPP; ref. 29) and surface PO_4 observations[9] with two adjustable coefficients, as described in the Supplementary Methods. The spatial dependence of γ, inherited from NPP and $[PO_4]_{obs}$, accounts for growth-limiting factors other than phosphate availability. Carbon uptake is modelled using

$$J_C = (C:P)_{exp} \cdot J_P$$

with a separate $(C:P)_{exp}$ parameter for each region shown in Fig. 1. A fraction δ of the production is routed to dissolved pools of organic phosphorus and carbon, which is regenerated with timescale κ^{-1}. The remaining fraction is exported by sinking particles with a flux profile $J(z) \propto (z/z_c)^{-b}$, where $z_c = -73.4$ m. In addition to organic carbon fluxes due to the formation and remineralization of particulate and dissolved organic carbon, the carbon model also includes air–sea fluxes of natural and anthropogenic CO_2, fluxes due to sinking $CaCO_3$ shells, and the concentrating and diluting effect of evaporation and precipitation. The fluxes of carbon due to sinking $CaCO_3$ shells introduces two further nuisance parameters in the model, the particulate inorganic to organic carbon ratio (R) and the e-folding remineralization length scale (d) for particulate inorganic carbon. The equilibrium model solutions are obtained efficiently by applying Newton's method to the steady-state equations[30]. A Bayesian inverse procedure is used to infer the most probable $(C:P)_{exp}$ values, taking into account the uncertainty in the nuisance parameters $\alpha, \beta, \delta, b, \kappa, R$ and d (see Supplementary Methods for complete details).

References

1. Redfield, A., Ketchum, B. H. & Richards, F. A. in *The Sea* Vol. 2 (ed. Hill, M. N.) 26–27 (Interscience, 1963).
2. Ito, T. & Follows, M. J. Preformed phosphate, soft tissue pump and atmospheric CO_2. *J. Mar. Res.* **63,** 813–839 (2005).
3. Moore, J. K., Lindsay, K., Doney, S. C., Long, M. C. & Misumi, K. Marine ecosystem dynamics and biogeochemical cycling in the Community Earth System Model CESM1(BGC): Comparison of the 1990s with the 2090s under the RCP4.5 and RCP8.5 scenarios. *J. Clim.* **26,** 929109312 (2013).
4. Bopp, L. *et al.* Multiple stressors of ocean ecosystems in the 21st century: Projections with CMIP5 models. *Biogeosciences* **10,** 6225–6245 (2013).
5. Martiny, A. C. *et al.* Strong latitudinal patterns in the elemental ratios of marine plankton and organic matter. *Nature Geosci.* **6,** 279–283 (2013).
6. Primeau, F. W., Holzer, M. & DeVries, T. Southern ocean nutrient trapping and the efficiency of the biological pump. *J. Geophys. Res.* **118,** 2547–2564 (2013).
7. DeVries, T. & Primeau, F. Dynamically- and observationally-constrained estimates of water-mass distributions and ages in the global ocean. *J. Phys. Oceanogr.* **41,** 2381–2401 (2011).
8. Key, R. M. *et al.* A global ocean carbon climatology: Results from Global Data Analysis Project (GLODAP). *Glob. Biogeochem. Cycles* **18** (2004).
9. Garcia, H. E. *et al.* in *NOAA Atlas NESDIS 71* Vol. 4 (ed. Levitus, S.) 398 (US Government Printing Office, 2010).
10. Emerson, S. Annual net community production and the biological carbon flux in the ocean. *Glob. Biogeochem. Cycles* **28,** 14–28 (2014).
11. Sarmiento, J. & Gruber, N. *Ocean Biogeochemical Dynamics* 503 (Princeton Univ. Press, 2006).
12. Takahashi, T., Broecker, W. & Langer, S. Redfield ratio based on chemical data from isopycnal surfaces. *J. Geophys. Res.* **90,** 6907–6924 (1985).

13. Anderson, L. A. & Sarmiento, J. L. Redfield ratios of remineralization determined by nutrient data analysis. *Glob. Biogeochem. Cycles* **8,** 65–80 (1994).
14. Li, Y-H. & Peng, T-H. Latitudinal change of remineralization ratios in the oceans and its implication for nutrient cycles. *Glob. Biogeochem. Cycles* **16,** 1130 (2002).
15. Schneider, B., Karstensen, J., Oschlies, A. & Schlitzer, R. Model-based evaluation of methods to determine C:N and N:P regeneration ratios from dissolved nutrients. *Glob. Biogeochem. Cycles* **19,** GB2009 (2005).
16. Gebbie, G. & Huybers, P. 'How is the ocean filled?' *Geophys. Res. Lett.* **38,** L06604 (2011).
17. Martiny, A. C., Vrugt, J. A., Primeau, F. W. & Lomas, M. W. Regional variation in the particulate organic carbon to nitrogen ratio in the surface ocean. *Glob. Biogeochem. Cycles* **27,** 723–731 (2013).
18. Deutsch, C. & Weber, T. Nutrient ratios as a tracer and driver of ocean biogeochemistry. *Annu. Rev. Mar. Sci.* **4,** 113–141 (2012).
19. Wu, J. F., Sunda, W., Boyle, E. A. & Karl, D. M. Phosphate depletion in the western North Atlantic Ocean. *Science* **239,** 759–762 (2000).
20. Lomas, M. W. *et al.* Sargasso Sea phosphorus biogeochemistry: An important role for dissolved organic phosphorus (DOP). *Biogeosciences* **7,** 695–710 (2010).
21. Sohm, J. A., Webb, E. A. & Capone, D. G. Emerging patterns of marine nitrogen fixation. *Nature Rev. Microbiol.* **9,** 499–508 (2011).
22. Luo, *et al.* Database of diazotrophs in global ocean: Abundance, biomass and nitrogen fixation rates. *Earth Syst. Sci. Data* **4,** 47–73 (2012).
23. Moore, J. K. & Doney, S. C. Iron availability limits the ocean nitrogen inventory stabilizing feedbacks between marine denitrification and nitrogen fixation. *Glob. Biogeochem. Cycles* **21,** GB2001 (2007).
24. Guilderson, T. P., McCarthy, M. D., Dunbar, R. B., Englebrecht, A. & Roark, E. B. Late Holocene variations in Pacific surface circulation and biogeochemistry inferred from proteinaceous deep-sea corals. *Biogeosci. Discuss.* **10,** 3925–3949 (2013).
25. Laws, E. A., D'Sa, E. & Naik, B. Simple equations to estimate ratios of new or export production to total production from satellite derived estimates of sea surface temperature and primary production. *Limnol. Oceanogr. Methods* **9,** 593–601 (2011).
26. Westberry, T. K., Williams, P. J. le B. & Behrenfeld, M. J. Global net community production and the putative net heterotrophy of the oligotrophic oceans. *Glob. Biogeochem. Cycles* **22,** GB4019 (2012).
27. DeVries, T., Primeau, F. & Deutsch, C. The sequestration efficiency of the biological pump. *Geophys. Res. Lett.* **39,** L13601 (2012).
28. Steinacher, M. Projected 21st century decrease in marine productivity: A multi-model analysis. *Biogeosciences* **7,** 979–1005 (2010).
29. Westberry, T., Behrenfeld, M. J., Siegel, D. A. & Boss, E. Carbon-based primary productivity modeling with vertically resolved photoacclimation. *Glob. Biogeochem. Cycles* **26,** GB4019 (2008).
30. Kwon, E. Y. & Primeau, F. Optimization and sensitivity of a global biogeochemistry ocean model using combined *in situ* DIC, alkalinity, and phosphate data. *J. Geophys. Res.* **113,** C08011 (2008).

Author contributions

Y-C.T., F.W.P. and A.C.M. initiated this study. Y-C.T. and F.W.P. formulated the inverse problem and carried out the model inversions with advice from A.C.M. and J.K.M. M.W.L. provided the BATS sediment trap data. Y-C.T. and F.W.P. wrote the paper with input from A.C.M., J.K.M. and M.W.L.

Additional information

Supplementary information is available in the online version of the paper. Reprints and permissions information is available online at www.nature.com/reprints. Correspondence and requests for materials should be addressed to F.W.P.

Competing financial interests

The authors declare no competing financial interests.